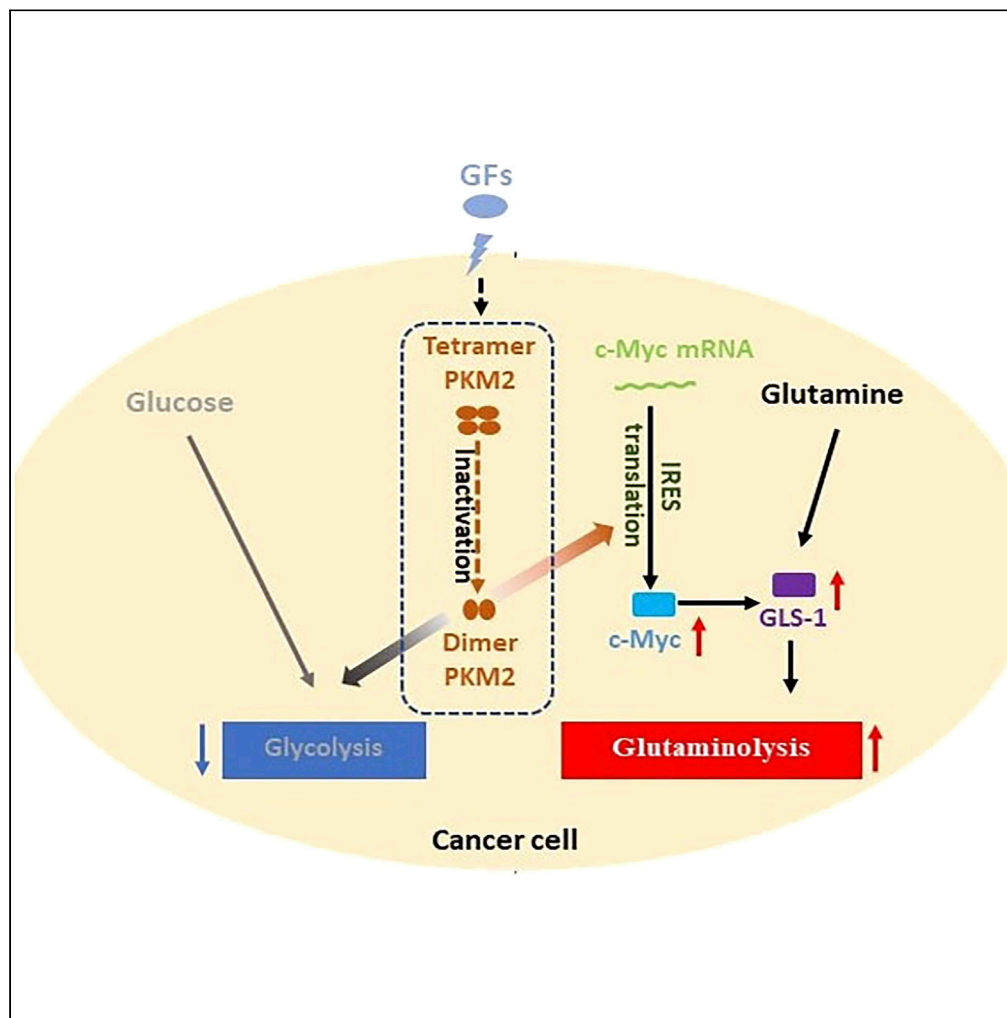


Article

Pyruvate Kinase M2 Coordinates Metabolism Switch between Glycolysis and Glutaminolysis in Cancer Cells



Liangwei Li,
Guangda Peng,
Xiaowei Liu,
Yinwei Zhang,
Hongwei Han, Zhi-
Ren Liu

zliu8@gsu.edu

HIGHLIGHTS

PKM2 coordinates cancer cell glucose and glutamine metabolism under growth stimulations

PKM2 controls cancer cell metabolism by regulating GLS and c-myc expression

PKM2 regulates c-Myc IRES-dependent translation

PKM2 dimer facilitates assembly of hnRNP K/L into c-Myc IRES complex

Li et al., iScience 23, 101684
November 20, 2020 © 2020
The Authors.
<https://doi.org/10.1016/j.isci.2020.101684>



Article

Pyruvate Kinase M2 Coordinates Metabolism Switch between Glycolysis and Glutaminolysis in Cancer Cells

Liangwei Li,^{1,2} Guangda Peng,^{1,2} Xiaowei Liu,¹ Yinwei Zhang,¹ Hongwei Han,¹ and Zhi-Ren Liu^{1,3,*}

SUMMARY

Cancer cells alter their nutrition metabolism to cope the stressful environment. One important metabolism adjustment is that cancer cells activate glutaminolysis in response to the reduced carbon from glucose entering into the TCA cycle due to inactivation of several enzymes in glycolysis. An important question is how the cancer cells coordinate the changes of glycolysis and glutaminolysis. In this report, we demonstrate that the pyruvate kinase inactive dimer PKM2 facilitates activation of glutaminolysis. Our experiments show that growth stimulations promote PKM2 dimer. The dimer PKM2 plays a role in regulation of glutaminolysis by upregulation of mitochondrial glutaminase I (GLS-1). PKM2 dimer regulates the GLS-1 expression by controlling internal ribosome entry site (IRES)-dependent c-myc translation. Growth stimulations promote PKM2 interacting with c-myc IRES-RNA, thus facilitating c-myc IRES-dependent translation. Our study reveals an important linker that coordinates the metabolism adjustment in cancer cells.

INTRODUCTION

An important molecular signature of cancer development and progression is that a shift in expression of isoenzymes of pyruvate kinase occurs to the tumor of almost all types. The tissue specific isoform (L, R, or M1) disappears. In replacement, PKM2 is expressed in cancer cells (Boros et al., 2002; Elbers et al., 1991; Hacker et al., 1998). Interestingly, PKM2 is converted to a pyruvate kinase inactivation dimer form from the more pyruvate kinase active tetramer in response to growth stimulation (Gao et al., 2012, 2013; Mazurek et al., 2005). It is believed that the inactive dimeric PKM2 actually provides a metabolic advantage for supplying precursors for biosynthesis (Ferguson and Rathmell, 2008; Hitosugi et al., 2009; Mazurek, 2007). The dilemma is that it is not sufficient to meet the needs of both energy and biosynthesis intermediates for the rapid growth solely by adjustment of glycolysis. Tumor cells often turn to glutaminolysis, a metabolism pathway which uses another abundant nutrition source glutamine (Cairns et al., 2011; Chen and Russo, 2012; Dang, 2010; DeBerardinis and Chandel, 2016; Yang et al., 2017). Indeed, it is well documented that glutaminolysis is upregulated in cancer cells of many types (DeBerardinis et al., 2007). Metabolism of glutamine, in addition to providing carbon frame for biosynthesis and TCA cycle intermediates, also provides reducing power by directly converting to glutathione (GSH), which is the most abundant antioxidant in mammalian cells in handling oxidative stress (Cairns et al., 2011; Gorrini et al., 2013; Lamonte et al., 2013). An important question is how cancer cells coordinate the activities of glycolysis and glutaminolysis to meet their growth needs.

RESULTS

PKM2 Dimer Facilitates Glutaminolysis in Cancer Cells

Since conversion of tetramer PKM2 to dimer PKM2 reduces the activity of the last step of glycolysis (Gao et al., 2012, 2013; Wong et al., 2013), which consequently affects the metabolism of glucose, glucose and glutamine are two most abundant nutrition sources, we asked whether PKM2 also plays a role in the glutamine metabolism. Thus, we measured the glutamine consumption in PKM2 knockdown SW480 cells. Interestingly, PKM2 knockdown (Figure S1A) largely reduced the glutamine consumption. Exogenous expression of wild-type PKM2 restored the glutamine metabolism, while expression of PKM1 could not restore the glutamine consumption in the cells (Figure 1A), suggesting a potential role of PKM2 in

¹Department of Biology, Georgia State University, 145 Piedmont Ave SE, Atlanta, GA 30303, USA

²These authors contributed equally

³Lead Contact

*Correspondence:

zliu8@gsu.edu

<https://doi.org/10.1016/j.isci.2020.101684>



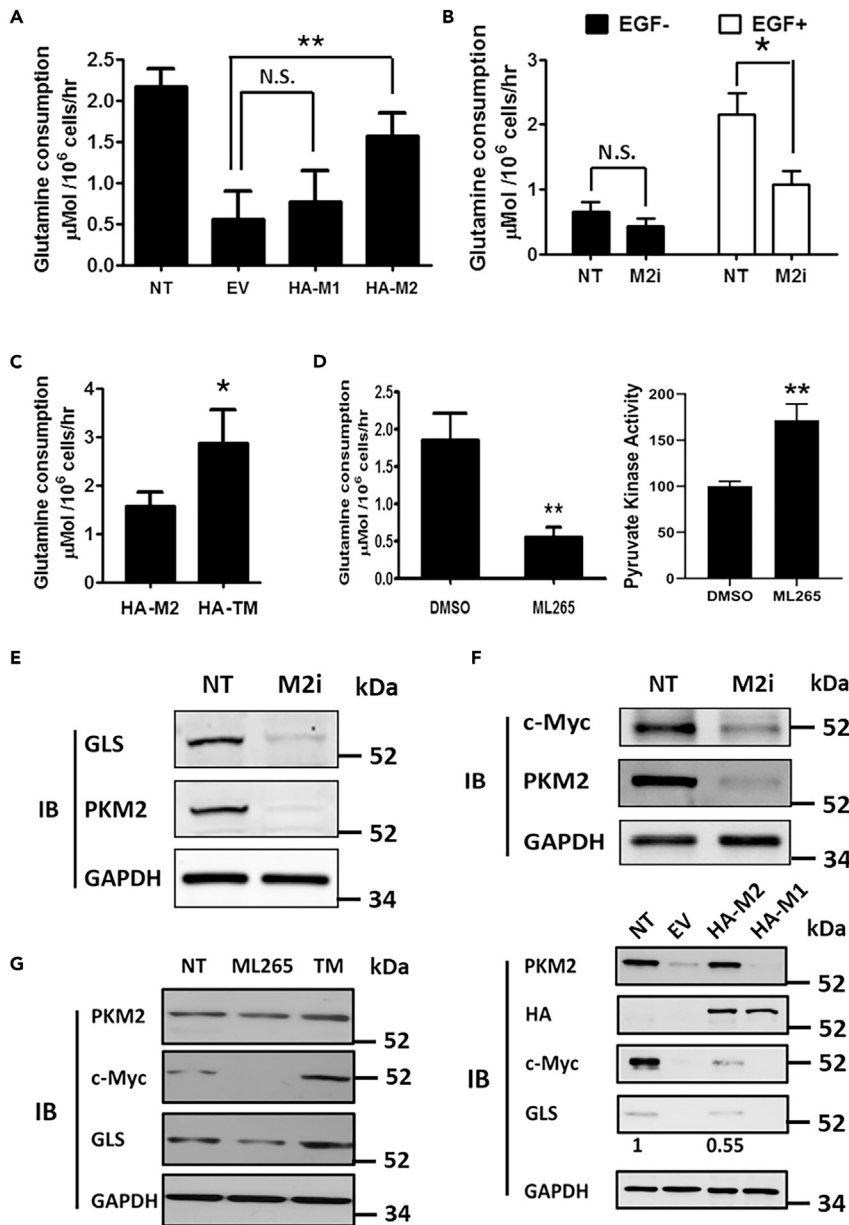


Figure 1. Dimer PKM2 Regulates Glutamine Metabolism

(A–C) and (D, left) Glutamine consumption in SW480 cells was measured by a commercial kit. The glutamine consumption is presented as $\mu\text{mole per million cells per hour}$. In (A–C), PKM2 was knocked down (M2i) or cells were treated by non-targeting siRNA (NT) as control. Wild-type PKM1 (HA-M1)/PKM2 (HA-M2), the TM mutant (HA-TM), or empty vector (EV) were expressed in the PKM2 knockdown cells. In (B), the cells were serum starving overnight prior to the treatment (EGF+) or no treatment (EGF-) with EGF.

In (D, left), the cells were treated with PKM2 activator ML265 (10 μM) or DMSO as control. Error bars represent mean \pm S.E.M. (D, right) Pyruvate kinase activity of extracts from SW480 cells treated with 10 μM ML265 was measured by the pyruvate kinase activity kit. The pyruvate kinase activity is presented as relative to the extracts of DMSO-treated cells (as 100) as reference.

(E–G) Cellular levels of PKM2 (IB:PKM2), glutaminase 1 (IB:GLS), and c-myc (IB:c-myc) were measured by immunoblot analyses. PKM2 was knocked down in the cells (M2i). Wild-type PKM1 (HA-M1)/PKM2 (HA-M2) or the TM mutant (HA-TM) was expressed in the PKM2 knockdown cells in (F) and (G). The cells were treated PKM2 activator ML265 (ML265) in (G). Immunoblot of HA-tag (IB: HA) indicates the levels of exogenous expression of PKM1/PKM2 and the TM mutant. Cells were treated with non-target siRNA (NT) as controls in (E), (F), and (G). Numbers under the GLS-1 blot panel in F indicate the relative band intensities quantitated by ImagingJ. Immunoblot of GAPDH in (E)–(G) is a loading control.

glutamine metabolism. It is demonstrated that growth stimulation activates glutaminolysis (DeBerardinis et al., 2008; Le et al., 2012; Wise et al., 2008). We examined the glutamine consumption in SW480 cells under epidermal growth factor (EGF) stimulation. The growth factor treatment increased the cell growth by over 3 folds (Figure S1B). In correlation to the cell proliferation, glutamine consumption increased almost 3 folds. Knockdown of PKM2 abolished the effects of the growth factor on increase of the glutamine consumption (Figure 1B). We previously reported that growth stimulation increased the dimer PKM2 in cancer cells (Gao et al., 2012, 2013). Thus, we question whether increase in dimer PKM2 upregulated glutamine consumption. We generated a PKM2 mutant with triple mutations (R399E, K422A, and N523A, referred to as TM mutant thereafter). Size-exclusion chromatography analyses indicated that the recombinant TM mutant mainly existed as a dimer (Figure S1C). We then asked if expression of this PKM2 TM mutant would increase glutamine consumption. Clearly, exogenous expression of the TM mutant in cancer cells (Figure S1D) increased glutamine consumption by over 2 folds compared to the expression of wild-type PKM2 (Figure 1C). This dimer PKM2 TM mutant did not have pyruvate kinase activity (Figure S1E). PKM2 activator increase pyruvate kinase activity of the enzyme by converting PKM2 dimer to a tetramer (Anastasiou et al., 2012) (Figure 1D). We tested whether treatment of SW480 cells by the PKM2 activator would affect glutamine metabolism in the cells. It was evident that glutamine consumption decreased 4 folds by the PKM2 activator (Figure 1D). The results suggest that the dimer PKM2 facilitates glutaminolysis under growth stimulations.

PKM2 Dimer Facilitates Glutaminolysis by Regulation of c-myc IRES-Dependent Translation

We then sought to determine how the dimer PKM2 affected glutamine metabolism. Mitochondrial glutaminase I (GLS-I) is the enzyme that catalyzes the first step of glutaminolysis, and is a key enzyme in regulation of glutamine metabolism (Gao et al., 2009; Hensley et al., 2013; Jin et al., 2016; Pan et al., 2015). We therefore investigated whether knockdown of PKM2 affected the GLS-1 expression. Immunoblot analyses of mitochondrial extracts prepared from SW480 cells in which PKM2 was knocked down showed that the GLS-1 was downregulated upon PKM2 knockdown (Figure 1E). Exogenous expression of wt PKM2 could restore the GLS-1 expression but PKM1 could not (Figure 1F). Expression of the TM mutant in SW480 cells increased GLS-1, while treatment of the cells by the PKM2 activator decreased GLS-1 in the cells (Figure 1G), suggesting that the pyruvate kinase inactive PKM2 dimer played a role in regulation of GLS-1 expression. It is known that c-myc regulates glutaminolysis by controlling GLS-1 expression (Gao et al., 2009; Goetzman and Prochownik, 2018; Wise et al., 2008). We reasoned whether dimer PKM2 regulates glutaminolysis via regulation of c-myc expression. Knockdown of PKM2 downregulated c-myc expression. Expression of PKM2 but not PKM1 could restore c-myc expression in PKM2 knockdown cells (Figure 1F). Expression of the TM mutant increased c-myc expression (Figure 1G). Treatment cells with PKM2 activator decreased c-myc expression (Figures 2A and 1G). The results suggest that PKM2 dimer regulates glutaminolysis by controlling c-myc expression. We then analyzed the function of PKM2 in regulation c-Myc/GLS expression and glutamine consumption in a human breast cancer cell line M4A4. EGF stimulation upregulated GLS/c-myc expression (Figure S2A) and increased glutamine consumption (Figure S2C). Knockdown of PKM2 decreased the cellular levels of c-myc and GLS (Figure S2B). Knockdown of PKM2 also abolished the effects of EGF in increasing glutamine consumption (Figure S2C). Results from M4A4 cells suggest that the function of PKM2 in regulating glutaminolysis via upregulation of c-Myc is not cancer type specific and is not specific to a particular cancer cell line. We asked how PKM2 dimer regulated c-myc expression. Reverse transcription polymerase chain reaction (RT-PCR) analyses of C-MYC pre-mRNA and mRNA in the PKM2 knockdown cells showed that PKM2 knockdown did not affect C-MYC pre-mRNA and matured mRNA levels (Figure 2B), suggesting PKM2 knockdown did not affect C-MYC mRNA transcription and processing. We speculated that PKM2 dimer regulated c-myc expression at the translation level. Two pathways contribute to c-myc protein synthesis: canonical cap-dependent translation and internal ribosome entry site (IRES)-dependent translation. The IRES-dependent c-myc translation is a pathway that is implicated in oncogenesis, particularly, the IRES-dependent c-myc translation remains active during apoptosis induction and G2/M transition of cell cycle when the canonical cap-dependent translation is largely suppressed (Chappell et al., 2000; Kim et al., 2003; Paulin et al., 1996; Subkhankulova et al., 2001; Thoma et al., 2004), suggesting a potential role of the IRES-dependent c-myc translation in cope with various cell stresses. Cap-analog m7G is an inhibitor that specifically inhibits cap-dependent translation with no effects on the IRES-dependent translation, while cycloheximide (CHX) inhibits all protein synthesis. Treatment of cells with CHX completely abrogated c-myc expression in cells while m7G only partially inhibited c-myc expression (Figures 2C and 2D). The inhibitory effects of m7G in the TM-mutant-expressing cells are less than those in cells without TM mutant expression (Figure 2D), suggesting that dimer PKM2 might regulate c-myc

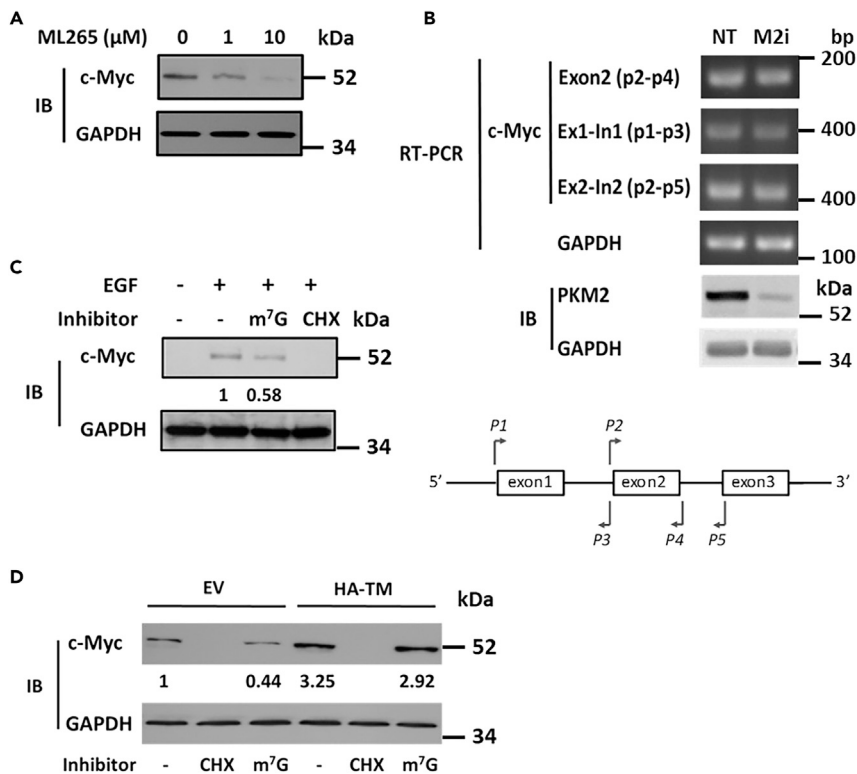


Figure 2. PKM2 Regulates c-myc Expression via Translational Control

(A) Cellular levels of c-myc (IB:c-Myc) were measured by immunoblot analyses in SW480 cells that are treated by indicated concentrations of PKM2 activator ML265.

(B) Cellular c-Myc pre-mRNA and mRNA levels were probed by RT-PCR using primer pairs showing at bottom of the panels. PKM2 was knocked down (M2i) or cells were treated with non-target siRNA (NT) as control. Immunoblot of PKM2 (IB:PKM2) indicates cellular levels of PKM2.

(C and D) Cellular levels of c-myc (IB:c-myc) were measured by immunoblot. Cells were treated (+) or untreated (–) with EGF. Cells were also treated with the Cap analog m7G or CHX as a translation inhibitor. In (D), PKM2 was knocked down, and the TM mutant (HA-TM) or empty vector (EV) was expressed in PKM2 knockdown cells. The numbers under each panel are quantitation of IB bands using ImagingJ. Immunoblot of GAPDH (IB:GAPDH) is a loading control for all immunoblot assays.

expression by IRES-dependent translation. To test this conjecture, bicistronic expression vectors were constructed containing open reading frame (ORFs) of HA-actin and green fluorescence protein (GFP) separated by c-myc IRES or Ith 5'-UTR (Figure 3A). A stop codon was placed after HA-actin ORF. There should be no GFP translation without IRES-mediated translation. The vectors were transfected into SW480 cells. Expression of GFP was monitored to assay c-myc IRES-dependent translation. Knockdown of PKM2 abrogated GFP expression (Figure 3B). To further test the role of PKM2 in regulating c-myc IRES-dependent translation, we probed the interaction of PKM2 with c-myc mRNA by RNA immunoprecipitation (RIP). Clearly, PKM2 interacted with c-myc mRNA in the IRES region (Figure 3C). Furthermore, RIP demonstrated that the PKM2 TM mutant also interacted with the c-myc IRES (Figure 3C). We also probed the interaction of PKM2 with mRNAs of the exogenously expressed bicistronic genes. Clearly, PKM2 interacted with the c-myc IRES in the bicistronic mRNA (Figure 3D). Furthermore, we isolated the complex assembled on the c-myc IRES. Protein contents in the isolated complex were identified by matrix-assisted laser desorption/ionization time-of-flight/time-of-flight (MALDI-tof/tof). Evidently, PKM2 was presented in the isolated c-myc IRES complex (Figure 3F). We conclude from our experiments that PKM2 regulates c-myc expression by the IRES-dependent translation and PKM2 interacts with the c-myc IRES complex.

PKM2 Facilitates hnRNP L and hnRNP K Interacting with c-Myc IRES

How does PKM2 regulate c-myc IRES-dependent translation is an open question. To elucidate the possible mechanism, we carried out co-immunoprecipitation attempting to find PKM2 interacting partner.

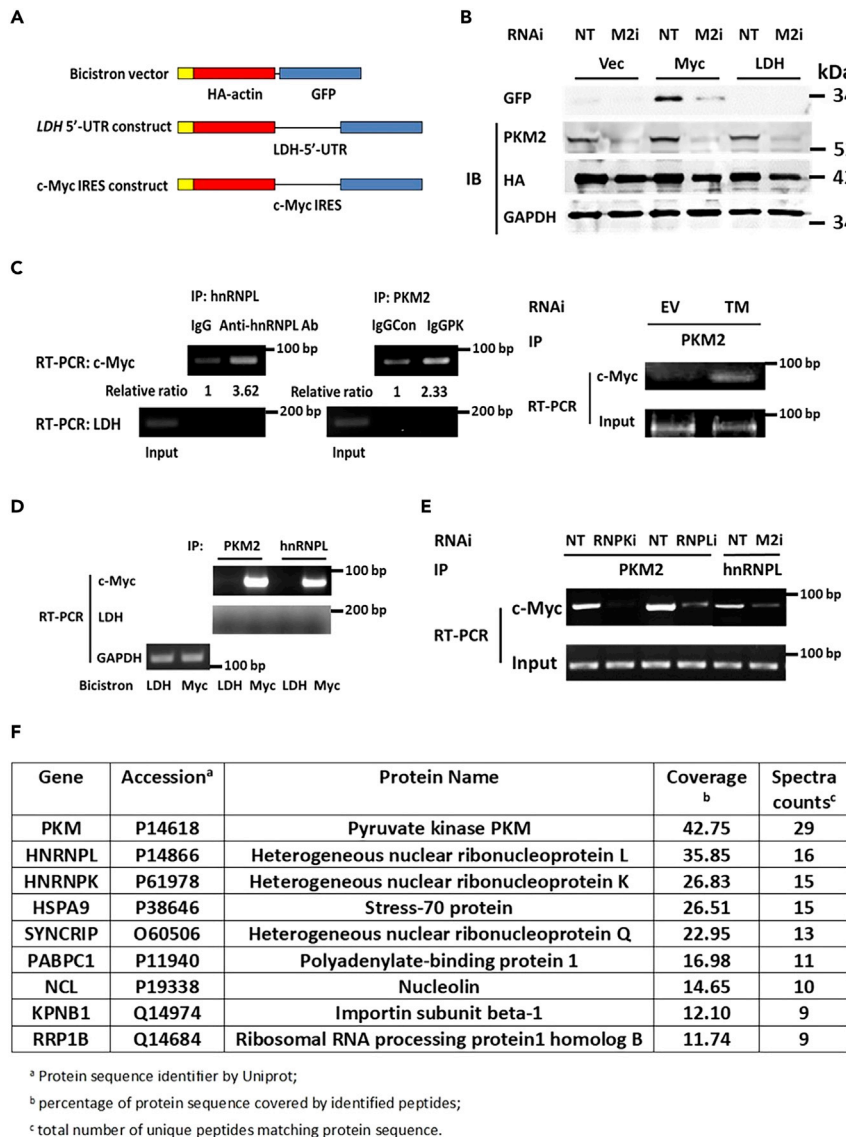


Figure 3. PKM2 Regulates c-myc Expression by IRES-Dependent Translation

(A) Diagram illustrates the construction of bicistronic vectors containing reading frames of HA-actin and GFP with 5'-UTR of *ldh* or *c-myc* IRES insertions between two reading frames.

(B) Cellular levels of GFP (IB:GFP) in the bicistronic vectors, Vec – no insertion, Myc – *c-myc* IRES as insertion, LDH, 5'-UTR of *ldh* as insertion, transfected cells. PKM2 was knocked down (M2i) or cells were treated with non-target siRNA (NT) as control. Immunoblots of PKM2 (IB:PKM2) and HA-actin (IB:HA) indicate cellular levels of PKM2 and HA-tagged proteins. Immunoblot of GAPDH (IB:GAPDH) is a loading control.

(C–E) RT-PCR analyses of RNA immunoprecipitation (RIP) of (C) cellular *c-Myc* mRNA using primer pair span *c-myc* IRES by antibodies against hnRNP L (left, IP:hnRNP L), PKM2 (middle, IP:PKM2), and PKM2 (right, IP: PKM2 for TM mutant).

(D) mRNAs from exogenously expressed bicistronic vectors in the cells (MYC, *c-myc* IRES, or LDH, *ldh*-5'-UTR) using primer pairs span *c-myc* IRES and GFP (*c-Myc*), 5'UTR of *ldh* and GFP (LDH) and (E) cellular *c-Myc* IRES RNA by antibodies against hnRNP L (IP: hnRNP L) and PKM2 (IP: PKM2).

Input in all RIP is a fraction of RT-PCR analyses of GAPDH mRNA of RNA extracts of the designated cells. In (C), IgG is a control antibody for anti-hnRNP L and IgGCon is a control for anti-PKM2 antibody IgGPK. Numbers under each top panel are relative band intensity quantified by ImagingJ. In (E), PKM2 (M2i), hnRNP L (RNPLi), or hnRNP K (RNPKi) were knocked down or cells were treated with non-target siRNA (NT) as control.

(F) List of proteins that co-precipitated down with *c-myc* IRES analyzed by ms-MOLDI-tof/tof. The number of peptides and percent of amino acid sequence matching the corresponding genes is indicated.

Interestingly, hnRNP L co-immunoprecipitated with PKM2 in SW480 extracts (Figure S3A). The co-immunoprecipitation was RNA independent (Figure S3B), which excluded a possibility that the co-immunoprecipitation (co-IP) was due to precipitation of large RNP complexes. The co-IP was verified by using anti-hnRNP L antibody (Figure S3C). MALDI-tof/tof analyses of the co-precipitates with the c-myc IRES complex also revealed that PKM2, hnRNP L, and hnRNP K are present in the c-Myc IRES complex (see Figure 3F). In consistent, hnRNP L interacted with c-myc IRES by RIP (see Figures 3C and 3D). It is well known that hnRNP K and hnRNP L functions in the c-myc IRES-dependent translation by modulating the IRES-RNA structure (Godet et al., 2019; Vaklavas et al., 2015). Knockdown of hnRNP L reduced cellular GLS-1 levels and decreased glutamine consumption, while exogenous expression of c-myc could restore the GLS-1 levels and glutamine consumption (see Figures 4C and 4D), suggesting that hnRNP L plays a role in regulation of glutaminolysis by IRES-dependent c-myc expression. We reasoned whether PKM2 regulated c-myc IRES-dependent translation by controlling the hnRNP L/K and c-myc IRES interaction. The hnRNP L interacted with c-myc IRES. However, knockdown of PKM2 reduced the interaction of hnRNP L with the c-Myc IRES (Figure S3D), and expression of the TM mutant in hnRNP L knockdown cells could not rescue the effects of hnRNP L knockdown on c-myc expression (Figure S3E). Interestingly, knockdown of hnRNP L/hnRNP K also abrogates the interaction of PKM2 with the c-myc IRES (see Figure 3E). It is possible that PKM2 and hnRNP L/hnRNP K cooperatively interact with the c-MYC IRES-RNA. Thus, our experiments support a mechanism that dimer PKM2 promotes assembly of an active complex on the c-myc IRES, including hnRNP L, hnRNP K, PKM2, and possibly other molecules, to facilitate the c-myc IRES-dependent translation.

PKM2 Dimer Confers Cancer Cells Glutamine Addiction

If dimer PKM2 mediates the effects of growth stimulation in activating glutaminolysis by promoting c-myc IRES-dependent translation, we expect that growth stimulations would upregulate c-myc and GLS-1 expression, and the regulatory effects would be PKM2 dependent. Indeed, c-myc and GLS-1 expression in SW480 cells was upregulated upon EGF and fibroblast growth factor (FGF) stimulations (Figure 4A). Up-regulation of c-myc and GLS-1 by EGF was dependent on PKM2 (Figure 4B). If c-myc IRES-dependent expression mediated the effects of PKM2 in regulation of GLS-1, we would expect that exogenous expression of c-myc would “rescue” the effects of PKM2 knockdown. Evidently, exogenous expression of c-myc in PKM2 knockdown cells restores the GLS-1 expression (Figure 4C) and glutamine consumption (Figure 4D). Furthermore, growth stimulations supposed to promote PKM2 and c-myc IRES-RNA interaction. We probed the PKM2 and c-myc IRES-RNA interaction by RIP in cells under EGF treatment. EGF treatment increased PKM2 and the c-myc IRES-RNA interaction (Figure 4E). The pattern of changes of the PKM2-IRES interaction was consistent with the GLS-1 expression under EGF stimulation (compare Figures 4E to 4A). PKM2 dimer mediates effects of growth signals in regulating glutaminolysis. We would expect different effects of PKM2 in glutamine consumption in cells under growth stimulation vs non-growth stimulation. Indeed, knockdown of PKM2 exerted stronger effects on glutamine consumption under EGF treatment vs non-treatment (see Figure 1B).

Upregulation of glutaminolysis commits cancer cells to glutamine addiction (Wise et al., 2008; Wise and Thompson, 2010). If dimer PKM2 upregulated glutaminolysis, it would be expected that increase in PKM2 dimer would lead to increase in the cells to glutamine addiction. Thus, we examined viability of SW480 cells with/without the TM mutant expression and PKM2 activator treatment under normal culture conditions or the culture condition with glutamine withdraw. Expression of the TM mutant decreased viability of cells under glutamine withdraw from culture medium (Figure 4F), while the PKM2 activator increased the viability of the cells under glutamine withdraw (Figure 4G). The fact that PKM2 dimer increases the cancer cell addiction to glutamine further support the functional role of PKM2 in coordinating the regulation of metabolism of glucose and glutamine.

DISCUSSION

Proliferation cancer cells limit carbon flow from glucose to the TCA cycle by reducing pyruvate kinase activity. An advantage of this change is pooling of glycolytic intermediates to meet the needs of high demanding for biosynthesis in proliferation. Converting of tetramer PKM2 to a dimer partially fulfills this regulation. However, change only in glycolysis is not sufficient to meet the metabolic needs for cancer progression and proliferation. It is well known that cancer cells switch to glutamine as an essential nutrient to support survival and growth (Eagle, 1955). It is not well understood how cancer cells coordinate the switch of the metabolism pathways. We demonstrate here that PKM2, a glycolytic enzyme, plays a role in regulating

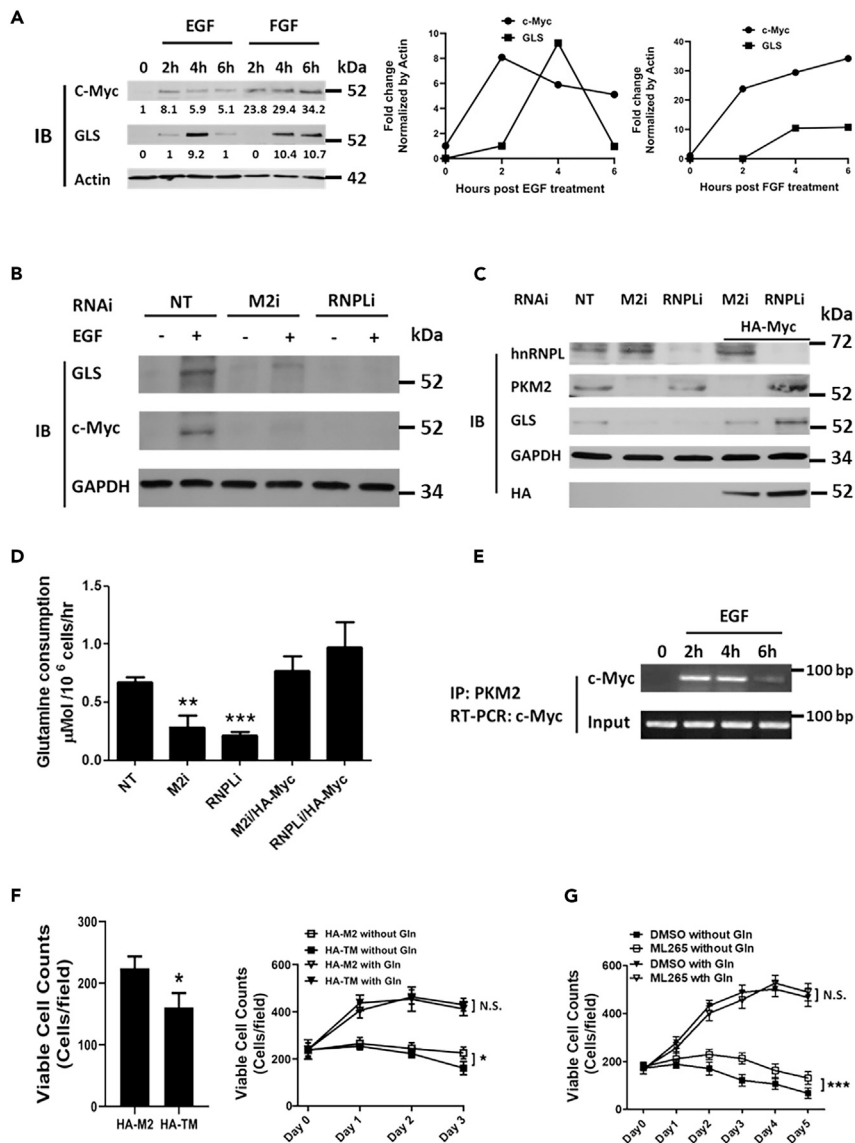


Figure 4. PKM2 Mediates Cancer Cell Glutamine Addiction under Growth Stimulation

(A–C) Cellular levels of c-myc (IB:c-myc), GLS1 (IB:GLS), hnRNP L (IB:hnRNP L), and PKM2 (IB:PKM2) are analyzed by immunoblots (A left, B and C). The cells are under indicated treatments. In (A), the cells were treated with EGF (50 ng/mL) and FGF (20 ng/mL). (A left panel) Numbers under the GLS and c-Myc blots indicate the band intensities relative to band intensities of actin blots quantitated by ImagingJ. (A, Right panels) The relative changes of cellular levels of c-myc and GLS1 over times. Immunoblots of GAPDH and β -actin are loading controls. Immunoblot of HA-tag indicates cellular levels of exogenously expressed HA-c-myc.

(D) Glutamine consumption in SW480 cells was measured by a commercial kit. The glutamine consumption is presented as $\mu\text{mole per million cells per hour}$. The cells are under indicated RNAi treatments, or HA-c-myc is exogenously expressed in the indicated RNAi treatment cells.

(E) RT-PCR analyses of RNA immunoprecipitation (RIP) of cellular c-Myc mRNA using PCR primer pair span c-Myc IRES by anti-PKM2 antibody (IP:PKM2). Input is a fraction of RT-PCR analyses of GAPDH mRNA in the RNA extracts of the cells. The cells were treated by EGF at indicated time points.

(F and G) Viability of SW480 cells with (with Gln) or without (without Gln) glutamine in medium was measured by cell counting (per view field). PKM2 wild-type (HA-PKM2) or TM mutant (HA-TM) was expressed in the cells in (F). Left panel in (F) is the cell viability measured at day 3 of culture. The cells were either treated with ML265 or DMSO as a control in (G). Error bars in D, F, and G represent mean \pm S.E.M.

glutamine metabolism. PKM2 dimer, glycolytic inactive form, activates glutaminolysis upon growth stimulation. The reciprocal roles of PKM2 in regulation of glycolysis and glutaminolysis function well in coordinating the switch of the metabolism in cancer cells. In addition to providing the carbon inputs for the TCA cycle to act as a biosynthetic base and alternative resources for NADPH and lipids, glutamate, the immediate product of glutamine in glutaminolysis, provides reducing power by directly converting to GSH, which is the most abundant anti-oxidant in mammalian cells (Cairns et al., 2011; Gorrini et al., 2013; Lamonte et al., 2013). An important metabolism role of PKM2 in cancer cells is help to cope with oxidative stress (Anastasiou et al., 2011). It is plausible that the upregulation of glutaminolysis by dimer PKM2 may help PKM2 to fulfill the role.

Regulation of c-myc IRES-dependent translation by dimer PKM2 is intriguing. C-myc regulates PKM2 expression by controlling PKM2 pre-mRNA splicing (David et al., 2010). As a feedback, PKM2 regulates c-MYC gene transcription (Luo et al., 2011) (Yang et al., 2011, 2012). We showed here another feedback loop that dimer PKM2 regulates c-myc translation. Regulation of c-myc IRES-dependent translation by dimer PKM2 allows quick response of cancer cells to adoption of various stress conditions. It is well established that cancer cells employ very different, yet co-existing, pathways to cope both hypoxia condition and cell proliferation needs. It is not well understood how cancer cells coordinate or “fine-tune” the opposite signal pathways to allow them to proliferate under stressful hypoxia conditions (Gordan et al., 2007). Hypoxia/Hif1 α and c-myc control PKM2 expression (David et al., 2010; Luo et al., 2011); PKM2 plays a role in regulation of Hif1 α activity (Luo et al., 2011; Palsson-McDermott et al., 2015). Furthermore, hypoxia and Hif1 α along with c-myc also regulate metabolism adjustment and glutaminolysis in cancer cells (Goetzman and Prochownik, 2018). Thus, it is plausible that the functional role of PKM2 in coordinating glycolysis and glutaminolysis switch and in regulating c-myc IRES-dependent translation is a critical control point for cancer cells to “fine-tune” cell responses to hypoxia environments.

Limitations of the Study

Our data demonstrate the regulation of c-myc expression by dimer PKM2 via the IRES-dependent translation. Although our data suggest that PKM2 facilitates assembly of hnRNP L/K into c-Myc IRES complex, further study is needed to elucidate how assembly of hnRNP L/K into c-Myc IRES complex facilitated by PKM2 controls assembly of c-Myc IRES complex. Furthermore, whether dimer PKM2 is directly involved in the IRES-dependent c-myc translation, e.g. recruiting translation initiation factors to the IRES and/or modulating c-Myc IRES structure, remain to be elucidated. It is shown that c-myc regulates expression and cellular functions of PKM2, including metabolism function of PKM2. PKM2 may also play a role in growth-signaling-related regulation of C-MYC expression at the gene transcription level. The relationship among these different regulatory events and consequential cellular responses needs further investigations.

Resource Availability

Lead Contact

Further information and requests for resources should be directed to and will be fulfilled by the Lead Contact, Zhi-Ren Liu (zliu8@gsu.edu).

Materials Availability

The study did not generate any unique reagents.

Data and Code Availability

This published article includes all data sets generated or analyzed during this study.

METHODS

All methods can be found in the accompanying [Transparent Methods supplemental file](#).

SUPPLEMENTAL INFORMATION

Supplemental Information can be found online at <https://doi.org/10.1016/j.isci.2020.101684>.

ACKNOWLEDGMENTS

We thank Chakra Ravi Turaga, H.H., and Malvika Sharma for excellent suggestions for our studies. We thank Ms. Birgit Neuhaus for her assistance in microscopic imaging. This work is supported in part by research

grants from the National Institutes of Health (CA175112, CA118113, CA178730) and Georgia Cancer Coalition to Z.-R.L.

AUTHOR CONTRIBUTIONS

Z.-R.L. conceptualized, planned, and coordinated the study. Z.-R.L. wrote the paper. L.L. and G.P. conducted most of experiments, data analyses, and participated in paper writing; X.L. conducted experiment of PKM2 and hnRNP L interaction and bicistronic vector construction and expression. Y.Z. conducted experiments of glutamine consumption and growth stimulation and analyses of c-myc expression. H.H. conducted some experiments. All authors discussed the results and commented on the paper.

DECLARATION OF INTERESTS

All authors declare no conflict interests.

Received: April 6, 2020

Revised: August 3, 2020

Accepted: October 12, 2020

Published: November 20, 2020

REFERENCES

- Anastasiou, D., Pouligiannis, G., Asara, J.M., Boxer, M.B., Jiang, J.K., Shen, M., Bellinger, G., Sasaki, A.T., Locasale, J.W., Auld, D.S., et al. (2011). Inhibition of pyruvate kinase M2 by reactive oxygen species contributes to cellular antioxidant responses. *Science* 334, 1278–1283.
- Anastasiou, D., Yu, Y., Israelsen, W.J., Jiang, J.K., Boxer, M.B., Hong, B.S., Tempel, W., Dimov, S., Shen, M., Jha, A., et al. (2012). Pyruvate kinase M2 activators promote tetramer formation and suppress tumorigenesis. *Nat. Chem. Biol.* 8, 839–847.
- Boros, L.G., Cascante, M., and Lee, W.N. (2002). Metabolic profiling of cell growth and death in cancer: applications in drug discovery. *Drug Discov. Today* 7, 364–372.
- Cairns, R.A., Harris, I.S., and Mak, T.W. (2011). Regulation of cancer cell metabolism. *Nat. Rev. Cancer* 11, 85–95.
- Chappell, S.A., LeQuesne, J.P., Paulin, F.E., deSchoolmeester, M.L., Stoneley, M., Soutar, R.L., Ralston, S.H., Helfrich, M.H., and Willis, A.E. (2000). A mutation in the c-myc-IRES leads to enhanced internal ribosome entry in multiple myeloma: a novel mechanism of oncogene deregulation. *Oncogene* 19, 4437–4440.
- Chen, J.Q., and Russo, J. (2012). Dysregulation of glucose transport, glycolysis, TCA cycle and glutaminolysis by oncogenes and tumor suppressors in cancer cells. *Biochim. Biophys. Acta* 1826, 370–384.
- Dang, C.V. (2010). Glutaminolysis: supplying carbon or nitrogen or both for cancer cells? *Cell Cycle* 9, 3884–3886.
- David, C.J., Chen, M., Assanah, M., Canoll, P., and Manley, J.L. (2010). HnRNP proteins controlled by c-Myc deregulate pyruvate kinase mRNA splicing in cancer. *Nature* 463, 364–368.
- DeBerardinis, R.J., and Chandel, N.S. (2016). Fundamentals of cancer metabolism. *Sci. Adv.* 2, e1600200.
- DeBerardinis, R.J., Mancuso, A., Daikhin, E., Nissim, I., Yudkoff, M., Wehrli, S., and Thompson, C.B. (2007). Beyond aerobic glycolysis: transformed cells can engage in glutamine metabolism that exceeds the requirement for protein and nucleotide synthesis. *Proc. Natl. Acad. Sci. U S A* 104, 19345–19350.
- DeBerardinis, R.J., Lum, J.J., Hatzivassiliou, G., and Thompson, C.B. (2008). The biology of cancer: metabolic reprogramming fuels cell growth and proliferation. *Cell Metab.* 7, 11–20.
- Eagle, H. (1955). The specific amino acid requirements of a human carcinoma cell (Stain HeLa) in tissue culture. *J. Exp. Med.* 102, 37–48.
- Elbers, J.R., van Unnik, J.A., Rijkse, G., van Oirschot, B.A., Roholl, P.J., Oosting, J., and Staal, G.E. (1991). Pyruvate kinase activity and isozyme composition in normal fibrous tissue and fibroblastic proliferations. *Cancer* 67, 2552–2559.
- Ferguson, E.C., and Rathmell, J.C. (2008). New roles for pyruvate kinase M2: working out the Warburg effect. *Trends Biochem. Sci.* 33, 359–362.
- Gao, P., Tchernyshyov, I., Chang, T.C., Lee, Y.S., Kita, K., Ochi, T., Zeller, K.I., De Marzo, A.M., Van Eyk, J.E., Mendell, J.T., et al. (2009). c-Myc suppression of miR-23a/b enhances mitochondrial glutaminase expression and glutamine metabolism. *Nature* 458, 762–765.
- Gao, X., Wang, H., Yang, J.J., Liu, X., and Liu, Z.R. (2012). Pyruvate kinase m2 regulates gene transcription by acting as a protein kinase. *Mol. Cell* 45, 598–609.
- Gao, X., Wang, H., Yang, J.J., Chen, J., Jie, J., Li, L., Zhang, Y., and Liu, Z.R. (2013). Reciprocal regulation of protein kinase and pyruvate kinase activities of pyruvate kinase m2 by growth signals. *J. Biol. Chem.* 288, 15971–15979.
- Godet, A.C., David, F., Hantelys, F., Tatin, F., Lacazette, E., Garmy-Susini, B., and Prats, A.C. (2019). IRES trans-acting factors, key actors of the stress response. *Int. J. Mol. Sci.* 20, 924.
- Goetzman, E.S., and Prochownik, E.V. (2018). The role for Myc in coordinating glycolysis, oxidative phosphorylation, glutaminolysis, and fatty acid metabolism in normal and neoplastic tissues. *Front. Endocrinol.* 9, 129.
- Gordan, J.D., Thompson, C.B., and Simon, M.C. (2007). HIF and c-Myc: sibling rivals for control of cancer cell metabolism and proliferation. *Cancer Cell* 12, 108–113.
- Gorrini, C., Harris, I.S., and Mak, T.W. (2013). Modulation of oxidative stress as an anticancer strategy. *Nat. Rev. Drug Discov.* 12, 931–947.
- Hacker, H.J., Steinberg, P., and Bannasch, P. (1998). Pyruvate kinase isoenzyme shift from L-type to M2-type is a late event in hepatocarcinogenesis induced in rats by a choline-deficient/DL-ethionine-supplemented diet. *Carcinogenesis* 19, 99–107.
- Hensley, C.T., Wasti, A.T., and DeBerardinis, R.J. (2013). Glutamine and cancer: cell biology, physiology, and clinical opportunities. *J. Clin. Invest.* 123, 3678–3684.
- Hitosugi, T., Kang, S., Vander Heiden, M.G., Chung, T.W., Elf, S., Lythgoe, K., Dong, S., Lonial, S., Wang, X., Chen, G.Z., et al. (2009). Tyrosine phosphorylation inhibits PKM2 to promote the Warburg effect and tumor growth. *Sci. Signal.* 2, ra73.
- Jin, L., Alesi, G.N., and Kang, S. (2016). Glutaminolysis as a target for cancer therapy. *Oncogene* 35, 3619–3625.
- Kim, J.H., Paek, K.Y., Choi, K., Kim, T.D., Hahm, B., Kim, K.T., and Jang, S.K. (2003). Heterogeneous nuclear ribonucleoprotein C modulates translation of c-myc mRNA in a cell cycle phase-dependent manner. *Mol. Cell. Biol.* 23, 708–720.
- Lamonte, G., Tang, X., Chen, J.L., Wu, J., Ding, C.K., Keenan, M.M., Sangokoya, C., Kung, H.N., Ilkayeva, O., Boros, L.G., et al. (2013). Acidosis induces reprogramming of

cellular metabolism to mitigate oxidative stress. *Cancer Metab.* 1, 23.

Le, A., Lane, A.N., Hamaker, M., Bose, S., Gouw, A., Barbi, J., Tsukamoto, T., Rojas, C.J., Slusher, B.S., Zhang, H., et al. (2012). Glucose-independent glutamine metabolism via TCA cycling for proliferation and survival in B cells. *Cell Metab.* 15, 110–121.

Luo, W., Hu, H., Chang, R., Zhong, J., Knabel, M., O’Meally, R., Cole, R.N., Pandey, A., and Semenza, G.L. (2011). Pyruvate kinase M2 is a PHD3-stimulated coactivator for hypoxia-inducible factor 1. *Cell* 145, 732–744.

Mazurek, S. (2007). Pyruvate kinase type M2: a key regulator within the tumour metabolome and a tool for metabolic profiling of tumours. *Ernst Schering Found. Symp. Proc.* 99–124.

Mazurek, S., Boschek, C.B., Hugo, F., and Eigenbrodt, E. (2005). Pyruvate kinase type M2 and its role in tumor growth and spreading. *Semin. Cancer Biol.* 15, 300–308.

Palsson-McDermott, E.M., Curtis, A.M., Goel, G., Lauterbach, M.A.R., Sheedy, F.J., Gleeson, L.E., van den Bosch, M.W.M., Quinn, S.R., Domingo-Fernandez, R., Johnston, D.G.W., et al. (2015). Pyruvate kinase M2 regulates Hif-1 α activity and IL-1 β induction and is a critical

determinant of the Warburg effect in LPS-activated macrophages. *Cell Metab.* 21, 347.

Pan, T., Gao, L., Wu, G., Shen, G., Xie, S., Wen, H., Yang, J., Zhou, Y., Tu, Z., and Qian, W. (2015). Elevated expression of glutaminase confers glucose utilization via glutaminolysis in prostate cancer. *Biochem. Biophys. Res. Commun.* 456, 452–458.

Paulin, F.E., West, M.J., Sullivan, N.F., Whitney, R.L., Lyne, L., and Willis, A.E. (1996). Aberrant translational control of the c-myc gene in multiple myeloma. *Oncogene* 13, 505–513.

Subkhankulova, T., Mitchell, S.A., and Willis, A.E. (2001). Internal ribosome entry segment-mediated initiation of c-Myc protein synthesis following genotoxic stress. *Biochem. J.* 359, 183–192.

Thoma, C., Bergamini, G., Galy, B., Hundsdoerfer, P., and Hentze, M.W. (2004). Enhancement of IRES-mediated translation of the c-myc and BiP mRNAs by the poly(A) tail is independent of intact eIF4G and PABP. *Mol. Cell* 15, 925–935.

Vaklavas, C., Meng, Z., Choi, H., Grizzle, W.E., Zinn, K.R., and Blume, S.W. (2015). Small molecule inhibitors of IRES-mediated translation. *Cancer Biol. Ther.* 16, 1471–1485.

Wise, D.R., DeBerardinis, R.J., Mancuso, A., Sayed, N., Zhang, X.Y., Pfeiffer, H.K., Nissim, I., Daikhin, E., Yudkoff, M., McMahon, S.B., et al. (2008). Myc regulates a transcriptional program that stimulates mitochondrial glutaminolysis and leads to glutamine addiction. *Proc. Natl. Acad. Sci. U S A* 105, 18782–18787.

Wise, D.R., and Thompson, C.B. (2010). Glutamine addiction: a new therapeutic target in cancer. *Trends Biochem. Sci.* 35, 427–433.

Wong, N., De Melo, J., and Tang, D. (2013). PKM2, a central point of regulation in cancer metabolism. *Int. J. Cell Biol.* 2013, 242513.

Yang, W., Xia, Y., Ji, H., Zheng, Y., Liang, J., Huang, W., Gao, X., Aldape, K., and Lu, Z. (2011). Nuclear PKM2 regulates beta-catenin transactivation upon EGFR activation. *Nature* 480, 118–122.

Yang, W., Zheng, Y., Xia, Y., Ji, H., Chen, X., Guo, F., Lyssiotis, C.A., Aldape, K., Cantley, L.C., and Lu, Z. (2012). ERK1/2-dependent phosphorylation and nuclear translocation of PKM2 promotes the Warburg effect. *Nat. Cell Biol.* 14, 1295–1304.

Yang, L., Venneti, S., and Nagrath, D. (2017). Glutaminolysis: a Hallmark of cancer metabolism. *Annu. Rev. Biomed. Eng.* 19, 163–194.

iScience, Volume 23

Supplemental Information

Pyruvate Kinase M2 Coordinates Metabolism

Switch between Glycolysis

and Glutaminolysis in Cancer Cells

Liangwei Li, Guangda Peng, Xiaowei Liu, Yinwei Zhang, Hongwei Han, and Zhi-Ren Liu

On-line supplementary materials

Reagents, Antibodies, and Cells are listed in the key resources table

Key Resources Table: Reagents, antibodies, and cell lines

| Reagents | Source | Identifier |
|--|--------------------------|-------------------|
| ML265 | Cayman Chemical | 13942 |
| Ultravision Peroxidase block | Thermo Fisher Scientific | TA060H2O2Q |
| Ultravision Protein block | Thermo Fisher Scientific | TA060PBQ |
| Antibody diluent OP Quanto | Thermo Fisher Scientific | TA-125-ADQ |
| Betazoid DAB Chromogen kit | Biocare Medical | BDB2004L |
| Tris Base | Fisher Scientific | BP154-1 |
| Tween-20 | Sigma-Aldrich | P5927 |
| Citrate buffer | Sigma-Aldrich | C9999-1000ML |
| Xylenes | Fisher Scientific | X5-4 |
| Ethanol | Decon Lab | 22032601 |
| DirectPCR Lysis Reagent (Mouse Tail) | Viagen Biotech | 102-T |
| PCR Master Mix | Thermo Scientific | F548S |
| 100bp DNA Ladder | Thermo Scientific | SM1143 |
| Molecular Biology Agarose | Bio-Rad | 1613101 |
| PKM2 siRNA | Thermo Fisher Scientific | s10575 |
| hnRNP L siRNA | Thermo Fisher Scientific | s6741 |
| hnRNP K siRNA | Thermo Fisher Scientific | s6739 |
| | | |
| | | |
| Antibodies | | |
| GLS1 | Proteintech | 19958-1-AP |
| c-myc | Thermo Fisher Scientific | 13-2500 |
| HA-tag | Abcam | ab9110 |
| GFP | Abcam | ab290 |
| hnPNP L | Abcam | ab6106 |
| GAPDH | Santa Cruz Biotechnology | sc-32233 |
| hnRNP K | Abcam | ab52600 |
| β -actin | Yurogen | MA5-18035 |
| | | |
| Chemicals, Peptides, and Recombinant Proteins | | |
| Recombinant murine EGF | | 236-EG |
| Recombinant murine FGF | | 233-FB |
| | | |
| Commercial Assay kits | | |

| | | |
|--|-----------|----------|
| Annexin V-FITC Apoptosis Staining Kit | abcam | ab14085 |
| BrdU Cell Proliferation Assay | Millipore | 2752 |
| Glutamine Colorimetric Assay Kit | Biovision | K556-100 |
| Experimental Models: Cell Lines | | |
| SW480 | ATCC | CCL-228 |

Primer sequence

| Name | sequence |
|--------------|---|
| c-Myc P1 | 5'-TCCAGCGAGAGGCAGAGGGGAGCGA-3' |
| c-Myc P2 | 5'-TCTGCGACCCGGACGACGAGACCT-3' |
| c-Myc P3 | 5'-GGCAAGTGGACTTCGGTGCTTACC-3' |
| c-Myc P4 | 5'-TGGAGGTGGAGCAGACGCTGTGGC-3' |
| c-Myc P5 | 5'-TTGACAGGCCTGGGCGGGCTTCG-3' |
| GLS1 F | 5'-GATGGGCAACAGTGTTAAG-3' |
| GLS1 R | 5'-CTCTCCCAGACTTTCCATTC-3' |
| c-Myc F | 5'-TGAGGAGACACCGCCAC-3' |
| c-Myc R | 5'-CATCGATTTCTTCCTCATCTTC-3' |
| Actin F | 5'-GAGCAAGAGAGGCATCCTC-3' |
| Actin R | 5'-GCACAGCCTGGATAGCAACG-3' |
| c-Myc-5UTR F | 5'-CAGGGTACCAATTCCAGCGAGAGGCAGAGG-3' |
| c-Myc-5UTR R | 5'-GTAGGATCCGCGTCGCGGGAGGCTGCTG-3' |
| LDH-5UTR F | 5'-CAGGGTACCTTAGTCTGATTTCCGCCACC-3' |
| LDH-5UTR R | 5'-GCAGGATCCGTGTCACACTACAGCTTCTTTAATGT-3' |

Transparent Methods.

Construction of PKM2 and the TM mutant, bicistronic, and HA-myc expression vectors:

PKM2 expression vector is the same of previous studies (Li et al., 2014; Zhang et al., 2016). PKM2 TM mutant was constructed based on PKM2 gene with three mutations on the following amino acid residues: R399E, K422A, N523A. Open reading frame of c-myc was cloned into pHM6 vector. These PKM2, PKM2 mutants, and PKM1 expression vector carry mutations at the PKM2 siRNA targeting site, therefore there are resistant to siRNA knockdown. For bicistronic vectors, β -actin ORF was synthesized and inserted into pEGFP-N1 vector with HA tag in N-terminal of

actin gene between HindIII and KpnI site by Epoch Life Science; Lactate dehydrogenase (LDH) gene 5'-UTR or c-Myc gene 5'-UTR was inserted by KpnI and BamHI.

Glutamine consumption measurement:

Intracellular glutamine consumption was measured by using commercially available assay kit from Biovision. Briefly, cell lysates were deproteinized by 10K Spin Column by centrifuging at 10,000 X g for 20 min at 4°C. Glutamate concentration [Glu] of the deproteinized samples was firstly determined. Glutamine was then converted to glutamate, and the total glutamate concentration [Glu_t] was measured again. Glutamine concentration was calculated based the equation of [Gln]=[Glu_t]-[Glu]. Cells were starved with glucose and glutamine for overnight. Fresh culture media containing 2mM D-Glutamine were applied to the cells on the second day for 2 hours and cells were lyzed at the indicated time points. Glutamine consumption was described by glutamine concentration changes Δ [Gln] per 10⁶ cells over time.

Biotinylation of c-Myc 5'-UTR

5'-UTR of c-Myc was biotinylated using MEGA short-script Kit (ThermoFisher). Firstly, the vector for 5'-UTR of c-Myc transcription is constructed using T7 RNA polymerase promoter sequence TAATACGACTCACTATAGGG from cellular 5'-UTR of c-Myc. For in vitro transcription, 2 μ l of reaction buffer, 2 μ l of 75mM ATP, 2 μ l of 75mM CTP, 2 μ l of 75mM GTP, 1.6 μ l of 75mM UTP, 0.4 μ l of 75mM Biotin-14-CTP, 2 μ l MEGAshortscript T7 enzyme and 200 ng of DNA template are mixed in water to a final volume 20 μ l in a PCR tube. The reaction was incubated at 37°C for 4 hours. DNA template was removed by DNase. Biotinylated C-myc IRES was purified by Ambion NucAway Spin column.

RNA-pulldown assay and RNA immunoprecipitation

SW480 cells cultured in the media containing EGF or buffer for 4 hours and cells were disrupted by polysome extraction buffer and the cell lysates were collected after centrifugation at highest speed for 10min. The cell lysates were incubated with biotinylated c-Myc IRES in assay buffer (20mM Tris-HCl pH 8.0, 1mM EDTA, 200mM NaCl and 1% triton X-100 containing protease inhibitor and RNA inhibitor) at 4°C for 4 hours. Then c-Myc IRES was pulled down by streptavidin-conjugated dynabeads, and dynabeads were washed three time with assay buffer without RNA inhibitor. Pull-down samples were treated with RNase and dynabeads were removed. The precipitates are subjected to further analyses.

Cell extracts were prepared using NE-PER Nuclear and Cytoplasmic Extraction reagents from ThermoFisher, containing RNase inhibitor and protease inhibitor cocktail. The cytoplasmic extracts were incubated with primary antibody and protein A/G dynabeads in assay buffer (20mM Tris-HCl pH 8.0, 2mM EDTA, 2mM DTT, 200mM NaCl and 0.5% NP-40 containing RNase inhibitor and protease inhibitor) at 4°C for overnight. On the second day, dynabeads were washed three time by assay buffer. The proteins immunoprecipitated by antibodies was subjected to western blot; RNAs precipitated with the target proteins were isolated by TRIzol RNA extraction reagent and analyzed by quantitative RT-PCR and real-time PCR.

Identification of c-MYC IRES interacting proteins by Mass Spectrometry

RNA-pulldown and IP samples proceeded to Trypsin digestion. Briefly, samples were concentrated by Vacuum concentrator and incubated in with 8M Urea and 5mM DTT at 37°C for 1 hour. 15mM iodoacetamide was applied to samples for 30min in the dark at room temperature.

The samples were trypsinized by Trypsin Gold from Promega in trypsin digestion buffer pH 8.0 at 37°C for overnight. The digested peptides were concentrated and desalted by C18 ZipTip pipette tips from Millipore. All HPLC-MS/MS experiments were performed on an Orbitrap Elite mass spectrometer equipped with NanoLC Ultimate 3000 high-performance liquid chromatography system.

Mass spectrometry data quantitative analysis

Mass spectrometry raw data files were analyzed by MaxQuant with Thermo Foundation 2.0. Data was analyzed according to previous study PMID19651621. Brief, relative protein abundance was estimated by the number of MS/MS spectral counts representing each identified protein. The quantitation of the spectral counts must meet three requirements: 1. Proteins with at least two unique peptides in three independent experiments were considered as positive partners; 2. Proteins must be identified in at two independent experiments; 3. The spectral count for a given protein in EGF treated group should be at least two folds higher than the one in buffer treated group; 4 The pvalue of the spectral counts for a given protein between EGF and buffer group should be <0.05.

Statistical calculations

Statistical analyses were carried out using the GraphPad Prism 6.0 software. All experiments were carried out in 5 times minimum. Statistical significance was assayed by either Student's t-test and/or one-way ANOVA for multiple comparisons followed by post-hoc Tukey's test. Box plots show range, median and quartiles. In all figures, *P < 0.05; **P < 0.01, ***P <

0.001, **** $P < 0.0001$; n.s. denotes not significant. All data are presented as mean \pm s.e.m. or as box plots.

Li, L., Zhang, Y., Qiao, J., Yang, J.J., and Liu, Z.R. (2014). Pyruvate kinase M2 in blood circulation facilitates tumor growth by promoting angiogenesis. *J Biol Chem* 289, 25812-25821.
 Zhang, Y., Li, L., Liu, Y., and Liu, Z.R. (2016). PKM2 released by neutrophils at wound site facilitates early wound healing by promoting angiogenesis. *Wound Repair Regen* 24, 328-336.

Supplementary Figure 1. Expression, pyruvate kinase activity, and dimer/tetramer status of PKM2 TM mutant. Related to Figure 1 and Figure 2

(A) Cellular levels of hnRNP L (IB:hnRNP L), hnRNP K (IB:hnRNP K), and PKM2 (IB:PKM2) were analyzed by immunoblot. The cells were treated with RNAi against hnRNP L (RNPLi), hnRNP K (RNPKi), PKM2 (M2i), and non-target RNAi (NT). Immunoblot of β -actin (IB:actin) is a control. (B) Proliferation of SW480 cells under 50 ng/ml EGF (+/-) treatment was analyzed by proliferation kit, and is presented as fold change (proliferation) by comparing to the cells before treatment. Error bars represent mean \pm S.E.M. (C) Chromatography profiles of TM mutant at concentrations of 20 μ M. Elution volumes equivalent to tetramer, dimer, and aggregation are indicated by arrows. (D) Cellular levels of PKM2 (IB:PKM2), exogenously expressed HA-TM (IB:HA) were analyzed by immunoblot in the extracts of cells expressing HA-TM or empty vector (EV). Immunoblot of GAPDH (IB:GAPDH) is a loading control. (E) Pyruvate kinase activity of recombinant PKM2 (rPKM2) and TM mutant (rPKM2 TM) was measured by the pyruvate kinase activity kit. The pyruvate kinase activity is presented as relative to the rPKM2 (as 100) as reference.

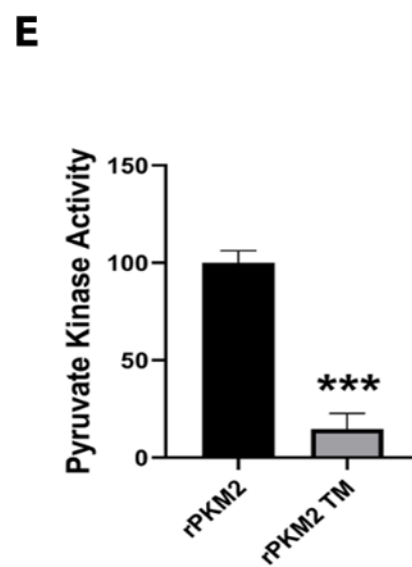
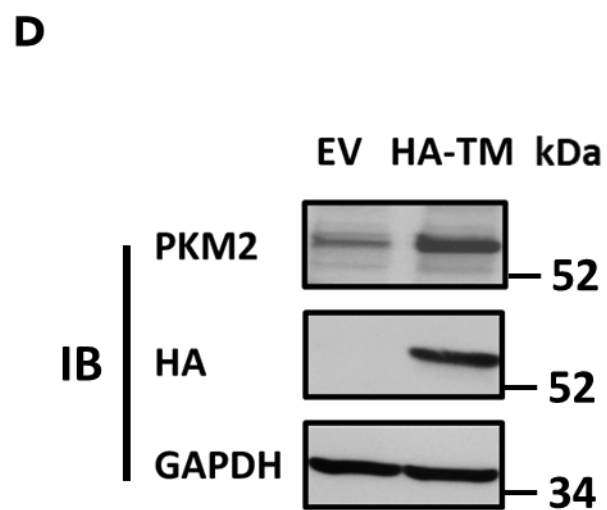
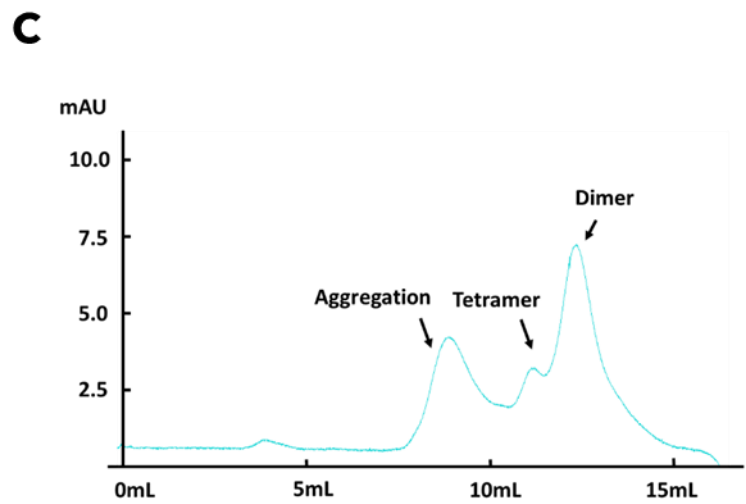
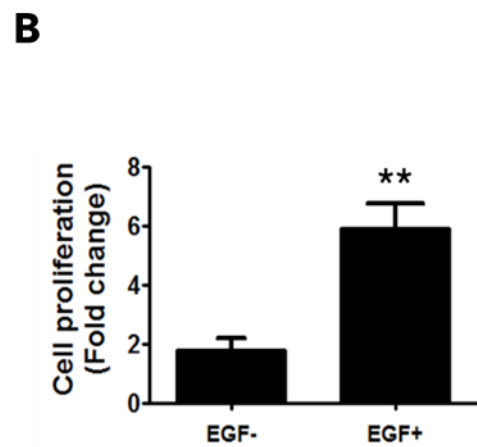
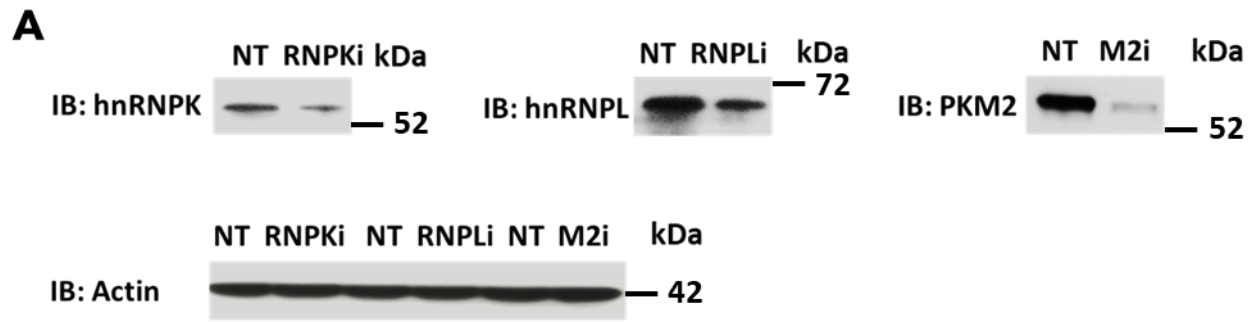
Supplementary Figure 2. PKM2 regulates c-myc and GLS expression and glutamine consumption in breast cancer M4A4 cells. Related to Figure 1.

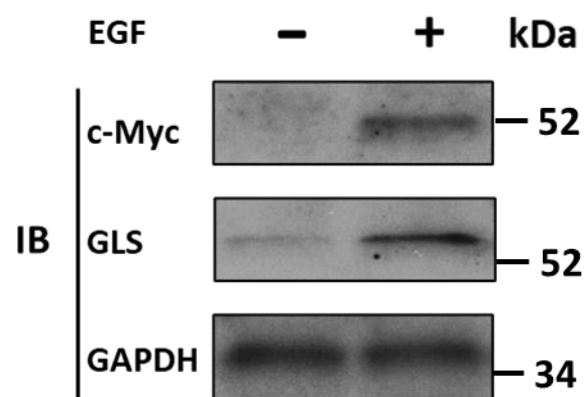
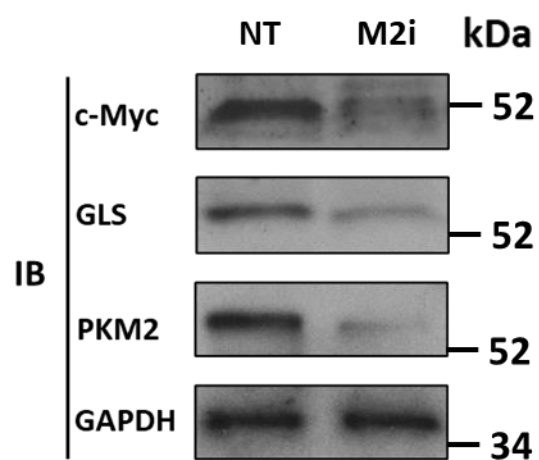
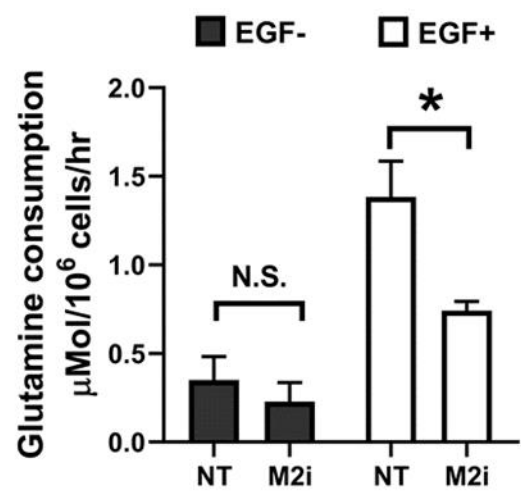
(A) and (B) Cellular levels of c-myc (IB:c-myc), GLS1 (IB:GLS), and PKM2 (IB:PKM2) were analyzed by immunoblot using indicated antibodies. Immunoblot of GAPDH (IB:GAPDH) is a

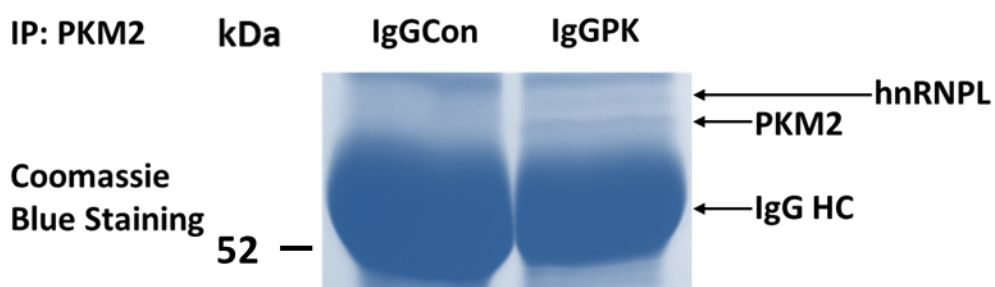
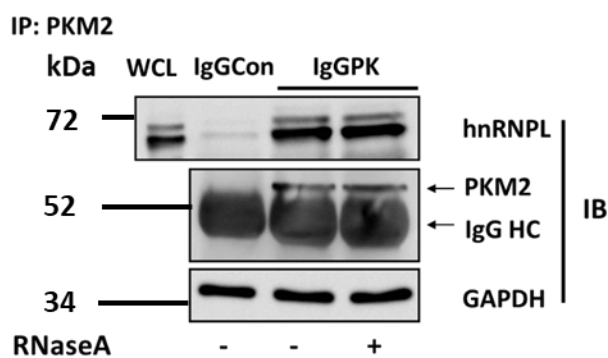
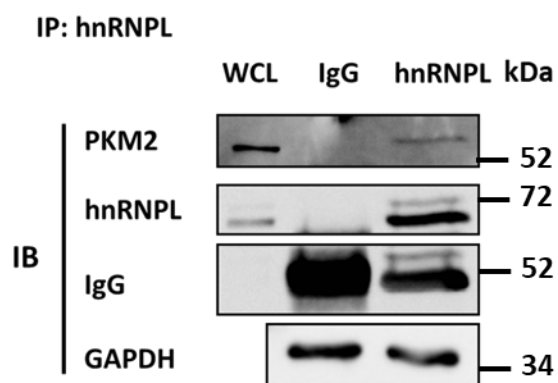
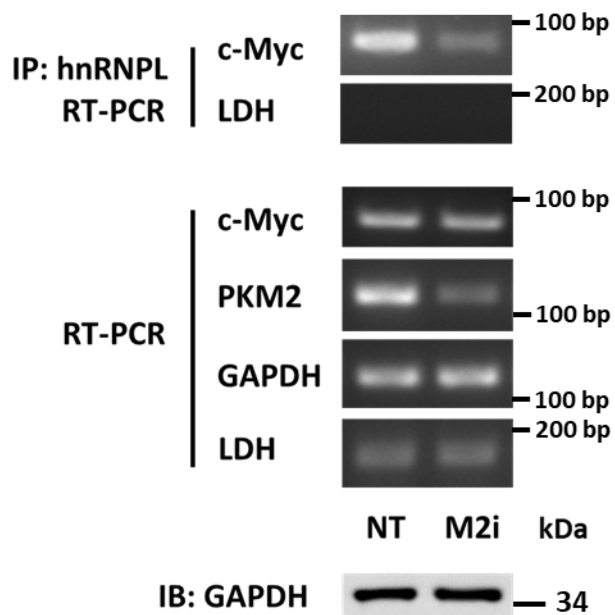
loading control. (C) Glutamine consumption in M4A4 cells was measured by commercial kit. The glutamine consumption is presented as $\mu\text{mole per million cells per hour}$. Error bars represent mean \pm S.E.M. In (A) & (C), the cells were serum starving overnight prior to the treatment (EGF+) or no treatment (EGF-) with EGF. In (B) & (C), PKM2 was knocked down (M2i) or cells were treated by non-targeting siRNA (NT) as control.

Supplementary Figure 3. PKM2 interacts with hnRNP L/K and c-Myc IRES. Related to Figure 3 &4.

(A) Representative image of Coomassie blue staining of SDS-PAGE of co-immunoprecipitation of PKM2 with hnRNP L using anti-PKM2 antibody (IgGPK). IgGCon is IgG purified from pre-bleeding of rabbit from which IgGPK was raised. PKM2, hnRNP L, and IgG heavy chain bands were indicated by the arrows. The hnRNP L and PKM2 bands were identified by ms-MALDI-tof/tof analyses. (B) and (C) Co-immunoprecipitation of PKM2 with hnRNP L using anti-PKM2 antibody (B, IP:PKM2) and anti-hnRNP L antibody (C, IP:hnRNPL). The extracts were treated by RNase A to remove RNA in the extracts in (B). IgG in (C) is mouse IgG as a control for anti-hnRNP L antibody. (D) (top) RT-PCR analyses of RNA immunoprecipitation (RIP) by antibodies against hnRNP L (IP:hnRNP L) of cellular mRNAs of c-Myc using primer pair span c-myc IRES (c-Myc) and LDH using primer pair span 5'-UTR of LDH mRNA (LDH). (bottom) RT-PCR analyses of cellular mRNA of c-myc, PKM2, GAPDH, and LDH. The cells were treated with RNAi against PKM2 (M2i) or non-target RNAi (NT). (E) Cellular levels of hnRNP L (IB:hnRNP L) and c-Myc (IB:c-Myc) were analyzed by immunoblots. The cells were treated by RNAi against hnRNP L (RNPLi) or non-target RNAi (NT). HA-tagged PKM2 TM mutant (HA-TM) was expressed in hnRNP L knockdown cells, indicating by immunoblot of HA (IB:HA). Immunoblot of GAPDH in (B), (C), (D), and (E) is a loading control.



A**B****C**

A**B****C****D****E**